Химическая технология

Chemical Technology

DOI: http://doi.org/10.20914/2310-1202-2024-3-209-216 Оригинальная статья/Research article

УДК 546.65.23.24 Open Access Available online at vestnik-vsuet.ru

Investigation of the Er-Sb-Te system

Saba H. Mamadova [1] saba.mammadova36@gmail.com 0000-0002-6545-2070
Fuad M. Sadigov [1] fuad.sadiqov.55@mail.ru 0009-0006-0571-6800
Zakir I. Ismailov [1] zakir-51@mail.ru 0000-0003-3499-953X
Kseniya B. Kim [2] kmkseniya@yandex.ru 0000-0001-5564-8267
Sabukhi I. Niftaliyev [2] sabukhi@gmail.com 0000-0001-7887-3061

1 Baku State University, 23 Zahid Khalilov street, Baku Az1148, Azerbaijan
2 Voronezh State University of Engineering Technologies, Revolution Av., 19 Voronezh, 394036, Russia

Abstract. Methods of physicochemical analysis, namely differential thermal analysis (DTA), high temperature differential thermal analysis (HTTA), X-ray phase analysis (XRD), microstructural analysis (MSA) and microhardness measurements are used to determine the nature of the physicochemical interaction in the Er-Sb-Te ternary system.. Phase diagrams of the following quasi-binary Er2Te3-Sb2Te3, ErTe-Sb2Te3, ErTe-SbTe, ErTe-Sb and non-quasi-binary Er-Sb2Te3, D (ErSb3Te5,5)-Te sections are presented for the first time. It has been established that at a component ratio of 1:1 in the Er2Te3-Sb2Te3 system, a new ternary phase with the composition ErSbTe3 is formed, which crystallizes in the hexagonal syngony with unit cell parameters: a=0.408; c=3.045 nm. In the system based on Sb_2Te_3, solid solutions are formed, the boundaries of which are up to 3 mol% Er_2Te_3 at room temperature, and at the eutectic temperature it reaches about 8 mol% Er_2Te_3. The ternary combination of $ErSbTe_3$ with an α-solid solution forms a eutectic, the coordinates of which are 20 mol % Er_2Te_3 and 800 K. The liquidus of the ErTe-Sb_2Te_3 system consists of two branches of primary crystallization of an α-solid solution based on Sb_2Te_3 and an Er_2Te_3 compound. In the ErTe-Sb_2Te_3 section, a region of homogeneity is also formed based on Sb_2Te_3 up to 5 mol % ErTe. The system state diagram is of the simple eutectic type. Eutectic coordinates 25 mol% ErTe and 850K. In the ErSb – ErTe and Sb – ErTe systems, no new ternary phases and homogeneity regions have been found. Eutectic coordinates in the ErSb – ErTe system; 50mol % ErTe and 1200K, and in the second system (Sb – ErTe) a degenerate eutectic is observed (at 900K). The cut Sb_2Te_3-Er intersects three, and D-Te two subordinate triangles. In both systems, ternary eutectic and peritectic invariant reactions occur at different temperatures. A projection of the liquidus surface of the Er-Sb-Te ternary system is also constructed, which consists of fourteen fields of primary crystallization of phases, separated by 25 monovariant equilibrium curves. Monovariant curves intersect at 11 nonvariant points, five of which are eutectic and six are peritectic.

Keywords: phase diagram, ternary system, phase equilibrium, quasi-binary, non-quasi-binary sections, solid solutions, liquidus of the system, crystallization of phases.

Исследование системы Er-Sb-Te

Саба Г. Мамадова [1] saba.mammadova36@gmail.com 0000-0002-6545-2070
Фуад М. Садыгов [1] fuad.sadiqov.55@mail.ru 0009-0006-0571-6800
Закир И. Исмаилов [1] zakir-51@mail.ru 0000-0003-3499-953X
Ксения Б. Ким [2] kmkseniya@yandex.ru 0000-0001-5564-8267
Сабухи И. Нифталиев [2] sabukhi@gmail.com 0000-0001-7887-3061

1 Бакинский государственный университет, ул. Захида Халилова 23, Баку, Az1148, Азербайджан
2 Воронежский государственный университет инженерных технологий, пр-т Революции, 19, г. Воронеж, 394036, Россия

Аннотация. Методами физико-химического анализа, а именно дифференциально-термического (ДТА), высокотемпературного дифференциально-термического (ВДТА), рентгенофазового (РФА), микроструктурного (МСА) анализов и измерением микротвердости определен характер физико-химического взаимодействия в тройной системе Er-Sb-Te. Впервые представлены фазовые диаграммы следующих квазибинарных Er_2Te_3-Sb_2Te_3, ErTe-Sb_2Te_3, ErTe-SbTe, ErTe-Sb и неквазибинарных Er-Sb_2Te_3, D ($ErSb_3Te_{5,5}$)-Te сечений. Установлено, что при соотношении компонентов 1:1 в системе Er_2Te_3-Sb_2Te_3 образуется новая тройная фаза составом ErSbTe3, которая кристаллизуется в гексагональной сингонии с параметрами элементарной ячейки: a=0,408; c=3,045 нм. В системе на основе Sb_2Te_3 образуются твердые растворы границы которых составляют до 3 мол% Er_2Te_3 при комнатной температуре, а при температуре эвтектики достигает около 8 мол% Er_2Te_3. Тройное соединение $ErSbTe_3$ с α-твердым раствором образует эвтектику, координаты которой составляют 20мол % Er_2Te_3 и 800К. Ликвидус системы ErTe-Sb_2Te_3 состоит из двух ветвей первичной кристаллизации α- твердого раствора на основе Sb_2Te_3 и соединения Er_2Te_3. В разрезе ErTe-Sb_2Te_3 также образуется область гомогенности на основе Sb_2Te_3 до 5 мол % ErTe. Диаграмма состояния системы относится к простому эвтектическому типу. Координаты эвтектики 25 мол% ErTe и 850К. В системах ErSb – ErTe и Sb – ErTe новые тройные фазы и области гомогенности не обнаружены. Координаты эвтектики в системе ErSb – ErTe; 50мол % ErTe и 1200К, а во второй системе (Sb – ErTe) наблюдается вырожденная эвтектика (при 900К). Разрез Sb_2Te_3- Er пересекает три, а D-Te два подчиненных треугольника. В обеих системах происходят тройные эвтектические и перитектические нонвариантные реакции при различных температурах. Также построена проекция поверхности ликвидуса тройной системы Er-Sb-Te, которая состоит из четырнадцати полей первичной кристаллизации фаз, разделенных 25 кривыми моновариантного равновесия. Моновариантные кривые пересекаются в 11нонвариантных точках, пять из которых являются эвтектическими и шесть перитектическими.

Ключевые слова: диаграмма состояния, тройная система, фазовое равновесие, квазибинарные, неквазибинарные сечения, твердые растворы, ликвидус системы, кристаллизация фаз.

Для цитирования
Мамадова С. Г., Садыгов Ф.М., Исмаилов З.И., Ким К.Б, Нифталиев С.И. Investigation of the Er-Sb-Te system // Вестник ВГУИТ. 2024. Т. 86. № 3. С. 209–216. doi:10.20914/2310-1202-2024-3-209-216

For citation
Mamadova S.H., Sadygov F.M., Ismailov Z.I., Kim K.B., Niftaliev S.I. Исследование системы Er-Sb-Te. Vestnik VGUIT [Proceedings of VSUET]. 2024. vol. 86. no. 3. pp. 209–216. (in Russian). doi:10.20914/2310-1202-2024-3-209-216

Introduction

Chalcogenides of antimony and bismuth are promising materials for optoelectronic devices [1, 2], solar cells [3], thermoelectric converters [4–6], photo electrochemical cells [7], optical recording [8], lithium-ion batteries [9, 10]. Moreover, they are also used as a topological insulator [11–13] and superconductors [13, 14].

According to [15, 16], one of the effective and promising ways to improve the thermoelectric properties of compounds is doping. It has recently been found that rare earth elements REE (REE = Lu, Ce, Sm, Er, La, Gd, etc.) can be successfully used as impurities to improve the thermoelectric characteristics of Bi_2Te_3 [17–28]. According to [27] the $Bi_{1.9}Gd_{0.1}Te_3$ composition is optimal for obtaining the maximum increase in ZT for Bi_2Te_3 compounds doped with REE.

The study of chemical interaction in Er-B-X (B-Sb, Bi; X-S, Se, Te) systems is of interest from the point of view of improving thermoelectric properties.

The phase diagrams boundary binary systems of the Er-Sb-Te ternary system have been studied in detail in [28–33].

In the Er-Te system, double compounds with compositions ErTe, Er_2Te_3, $ErTe_2$, $ErTe_3$ have been found.

System state diagram studied by Weissan. The Er + ErTe eutectic is at 13 at% Te and melts at 1270 °C. Between ErTe and Er_2Te_3 there is a continuous series of solid solutions. The melting points of the boundary compositions are 1325 and 1460 °C, respectively. Tritelluride $ErTe_3$ is formed by a peritectic reaction at 575 °C [28].

In the Sb-Te system at 618 °C, the congruently melting compound Sb_2Te_3 is formed. The solubility of Sb in Te is ~1 at. % at room temperature. The eutectic crystallizes at 92 at. % Te and 422 °C [29–31].

The Er-Sb system was studied by the authors [32–33] and the state diagram of the system was constructed. Two compounds with compositions ErSb and ErSb2 are formed in the system. The ErSb compound is formed at a ratio of components 1:1 with an open maximum at 1650 K, and $ErSb_2$ by the peritectic reaction:

$$L + ErSb \leftrightarrow ErSb_2 \ (975K)$$

ErSb forms a eutectic with Er, the eutectic coordinates are: 80 at.% Er and 1200 K [33].

Materials and methods

The initial materials for the synthesis of alloys were Er metal "Erm-O"; Sb "B-4"; Te "TA-2".

The alloys were obtained by direct alloying of the components in evacuated quartz ampoules at 900–1300K, depending on the composition, followed by slow cooling in a switched off furnace. To obtain an equilibrium state, the alloys were subjected to homogenizing annealing in evacuated quartz ampoules at temperatures 50–100 K below the solidus temperature for two weeks.

The study was carried out by a complex of methods of physical and chemical analysis.

Differential thermal analysis (DTA) was performed using an NTR-73 pyrometer and Thermoscan-2. The liquidus temperature of the high-temperature part of the diagrams was determined on a VDTA-8 in an inert atmosphere using W–W/Re thermocouples. Heating rate 40 deg./min.

X-ray diffraction analysis (XRD) was carried out by taking X-ray diffraction patterns of powders on a Bruker D8 ADVANCE diffractometer with Cu Kα radiation.

For microstructural analysis (microscope MIM-7), an etchant with the composition of 10% mol H_2SO_4 + 45g $K_2Cr_2O_7$ + 90 mol% H_2O was used. The etching process lasts 26 s. The microhardness of the alloys was measured on a PMT-3 microhardness tester at loads of 10 and 20 g. The measurement error was 1.2–1,43%.

Results

To study the chemical interaction in the entire concentration range and construct the projection of the liquidus surface of the Er-Sb-Te ternary system, the following sections were studied: ErSb-ErTe, Er_2Te_3-Sb_2Te_3, ErTe-Sb, ErTe-Sb_2Te_3, Sb_2Te_3-Er, and Sb_2Te_3 – D(ErSb3Te 5,5) Er_2Te_3-Sb_2Te_3 section is quasi-binary (Fig.1).

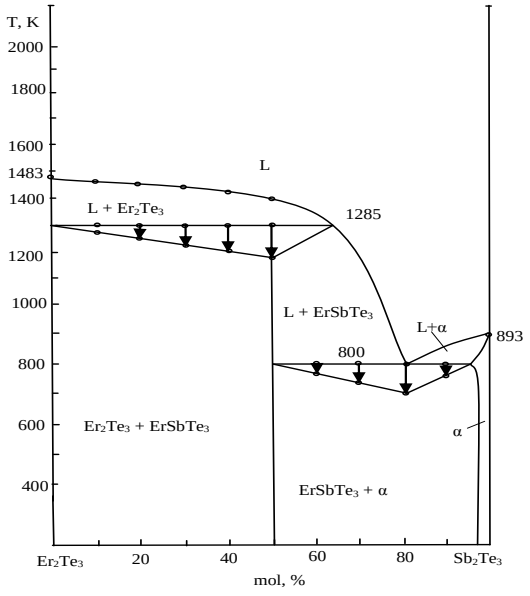

Figure 1. Phase diagram of the Sb_2Te_3-Er_2Te_3 system

It can be seen from the figure that the Sb_2Te_3-Er_2Te_3 section belongs to the simple eutectic type. At a ratio of components of 1:1, a ternary compound of composition $ErSbTe_3$ is formed in the system by a peritectic reaction at a temperature of 1285 K.

$$L + Er_2Te_3 \leftrightarrow ErSbTe_3$$

The $ErSbTe_3$ compound forms a eutectic with an α-solid solution based on Sb_2Te_3. Eutectic coordinates is 80 mol% Sb_2Te_3 and 800 K.

The formation of solid solutions based on Sb_2Te_3 was found, the boundary of which is approximately 3 mol.% Sb_2Te_3 at a temperature of 300 K.

By indexing the diffraction pattern of the 1:1 composition alloy, it was found that $ErSbTe_3$ crystallizes in a tetragonal syngony with unit cell parameters, a = 18.95Å; c = 12.68Å (Fiq.2)

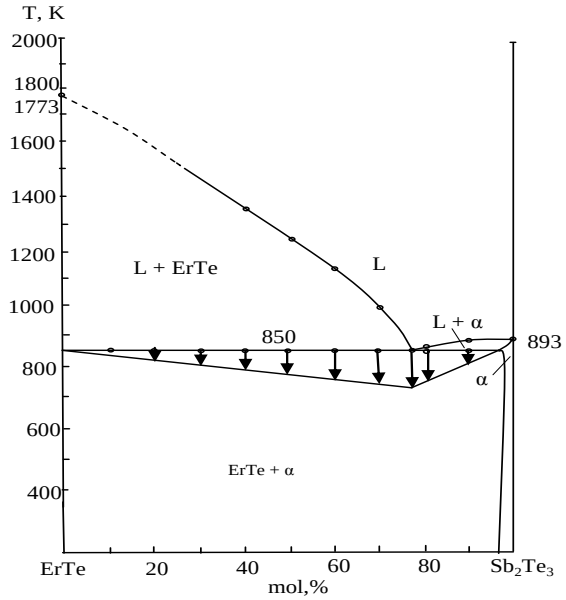

Figure 2. Phase diagram of the ErTe – Sb_2Te_3 system

Data on chemical interaction in sections of the eutectic type in the Er-Sb-Te system are given in Table 1.

Table 1.

The nature of the chemical interaction in sections

Sections	Eutectic coordinates		
	Sb_2Te_3 mol%	T, K	
Sb_2Te_3-ErTe	75	850	Fig.3
Sb-ErTe	degenerate	900	Fig.4
ErSb-ErTe	50	1200	Fig.5

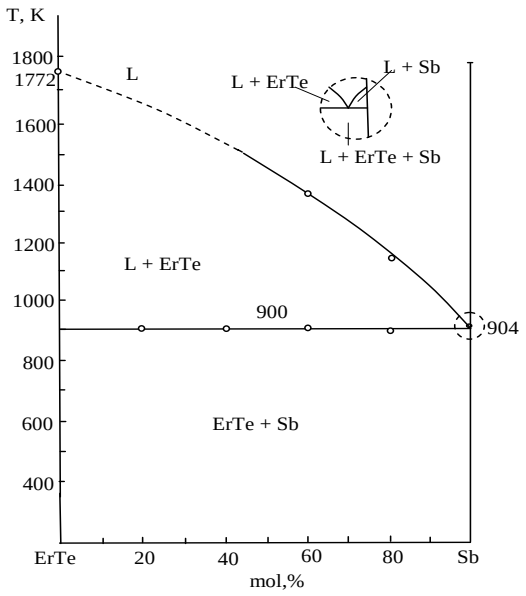

Figure 3. Phase diagram of the ErTe – Sb system

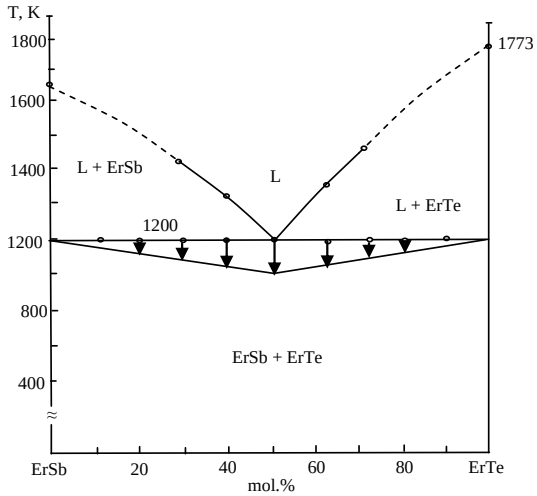

Figure 4. Phase diagram of the ErSb – ErTe – system

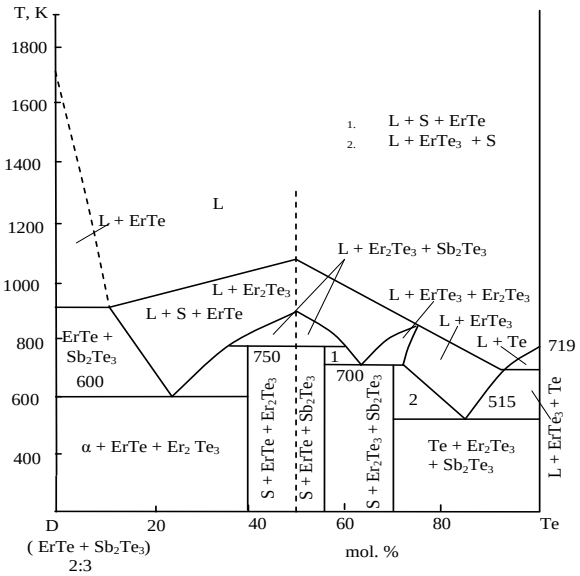

Figure 5. D(ErTe + Sb_2Te_3) – Te polythermal section of the phase diagram of the Er-Sb-Te system

Er-Sb_2Te_3 non-quasi-binary section (Fig. 2) crosses three subordinate triangles: ErSb-Er-ErTe, ErSb-Sb-ErTe, ErTe-Sb-Sb_2Te_3.

The effects at 1000 and 800 K reflect the co-crystallization of Er with ErTe and ErTe with an α-solid solution based on Sb2Te3, respectively.

Crystallization of the alloys of the part of the section of the intersecting triangle ErSb-Er-ErTe ends at a ternary eutectic temperature of 1600K, according to the reaction:

$$L \leftrightarrow ErSb + Er + ErTe$$

Peritectic transformations take place in this part of the system:

$$L + ErSb \leftrightarrow ErSb + ErTe \ (800\ K).$$

Part of the system crosses partial triangle III, where ternary eutectic and peritectic nonvariant transformations occur:

$$L + \alpha(Sb_2Te_3) \leftrightarrow \sigma + ErTe \ (765\ K)$$

$$L + \sigma \leftrightarrow \gamma + ErTe \ (700\ K)$$

$$L + \gamma \leftrightarrow \beta` + ErTe \ (650\ K)$$

$$L + Sb \leftrightarrow \beta + ErTe \ (750\ K)$$

$$L \leftrightarrow \alpha + \beta + ErTe \ (550\ K)$$

D($ErSb_3Te_{5,5}$) – Te section is non-quasi-binary (Fig. 7), crosses two triangles Sb_2Te_3-ErTe-Er_2Te_3 and Sb_2Te_3-Te-Er_2Te_3. Liquidus consists of four curves of primary phase crystallization: ErTe, Er_2Te_3, $ErTe_3$, and Te.

The following nonvariant eutectic and peritectic reactions take place in this part of the system:

$$L + Er_2Te_3 \leftrightarrow S + ErTe \ (750\ K)$$

$$L + Er_2Te_3 \leftrightarrow S + Sb_2Te_3 \ (750\ K)$$

$$L + S \leftrightarrow Er_2Te_3 + ErTe \ (700\ K)$$

$$L \leftrightarrow \alpha + ErTe + Er_2Te_3 \ (600\ K)$$

$$L \leftrightarrow Te + Er_2Te_3 + Sb_2Te_3 \ (515\ K)$$

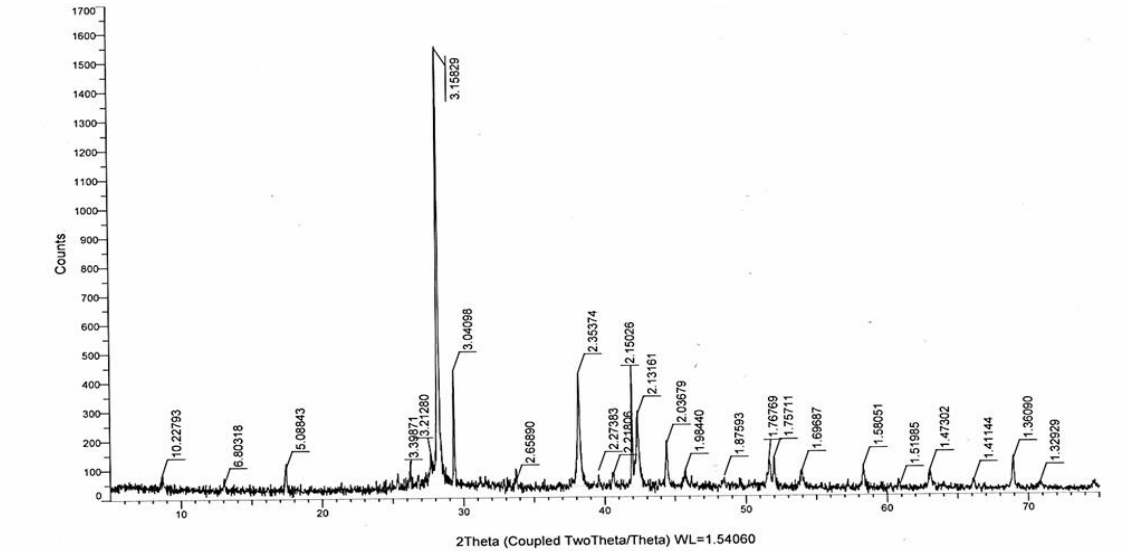

Figure 6. X-ray diffraction pattern of $ErSbTe_3$ compound

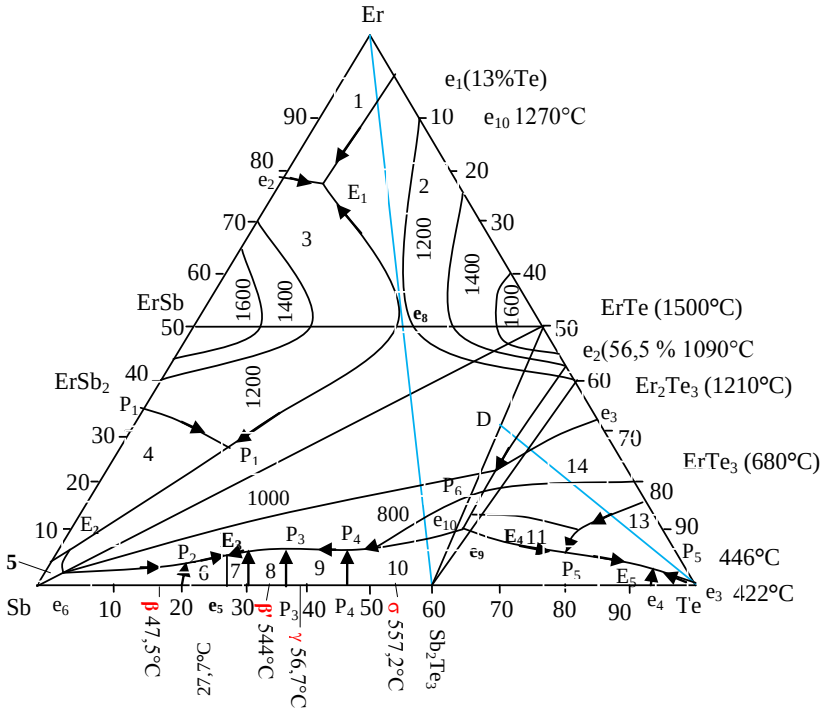

Figure 7. Liquidus surface projection of the Er-Sb-Te ternary system. Areas of primary crystallizations phases: 1 – Er, 2– ErTe, 3 – ErSb, 4 – $ErSb_2$, 5 – Sb, 6 – β, 7 – β`, 8 – h, 9 – σ, 10 – Sb_2Te_3, 11 – $ErSbTe_3$, 12 – Te, 13 – $ErTe_3$, 14 – Er_2Te_3

The study of the six sections described above and the literature data on binary systems made it possible to construct a projection of the liquidus surface of the Er-Sb-Te ternary system (Fig. 7). which can be divided into five secondary systems: ErSb-Er-ErTe, ErSb-Sb-ErTe, ErTe-Sb-Sb_2Te_3, Sb_2Te_3-ErTe-Er_2Te_3, Sb_2Te_3-Te-Er_2Te_3.

The liquidus of the investigated system consists of 14 primary phase crystallization fields separated by 25 monovariant equilibrium curves. The largest region of the diagram is occupied by the crystallization field of the ErTe compound (~55%). Monovariant curves intersect at 11 nonvariant points, 5 of which are eutectic and 6 are peritectic. Nonvariant reactions occurring during the crystallization of alloys are shown in Table 2.

Table 2.

Nonvariant equilibrium processes in the Er-Sb-Te ternary system

Point	Equilibria	Temperature T, K
e_{11}-E_1	L ↔ Er + ErSb	1200–60
e_1-E_1	L ↔ Er + ErTe	1343–600
$E_1e_8P_1$	L ↔ ErSb + ErTe	600–1200–800
P_1P_1	L ↔ ErSb + $ErSb_2$	975–800
P_1E_2	L ↔ $ErSb_2$ + Sb	800–695
$E_2e_6P_2$	L ↔ Er_2Te + Sb	675–900–850
$P_4e_{10}E_4$	L ↔ Sb_2Te_3 + ErTe	765–850–600
P_4P_4	L ↔ Sb_2Te_3 + σ	830–765
P_4P_3	L ↔ γ + ErTe	765–700
P_3P_3	L ↔ γ + β’	813–700
P_3E_3	L ↔ β’ + ErTe	700–550
e_5E_3	L ↔ β’+ γ	818–550
P_2P_2	L ↔ Sb + β	810–650
T_2E_3	L ↔ β + ErTe	750–650
e_2P_6	L ↔ ErTe + $ErTe_3$	1360–750
P_6E_4	L ↔ ErTe + $ErSbTe_3$(S)	750–600
$e_{19}E_4$	L ↔ ErTe + Sb_2Te_3	850–600
$P_6e_6P_6$	L ↔ $ErTe_3$ + S	760–1285–750
$E_4e_3P_5$	L ↔ Sb_2Te_3 + S	600–800–700
P_5P_6	L ↔ Er_2Te_3 + $ErTe_3$	923–750
P_6P_5	L ↔ S + $ErTe_3$	750–700
P_5E_5	L ↔ $ErTe_3$ + Sb_2Te_3	700–515

Conclusion

By using the DTA, HTDA, XRD, MSA and microhardness measurements the character of the physicochemical interaction in the Er-Sb-Te ternary system are studied. It has been established that the Sb_2 Te_3-Er_2 Te_3, Sb_2 Te_3-ErTe, ErTe-Sb, ErTe-ErSb sections are quasi-binary, while the Sb_2 Te_3-Er and D – Te sections are non-quasi-binary.

Литература

1 Baghbanzadeh-Dezfuli B., Jamali-Sheini F., Cheraghizade M. Sonical deposition of nanostructured Sb_2 Se_3 films for optoelectronic applications // Journal of Alloys and Compounds. 2021. V. 85. № 1. P. 157308. doi: 10.1016/j.jallcom.2020.157308

2 Wang F.K., Yang S.J., Zhai T.Y. 2D Bi_2 Se_3 materials for optoelectronics // IScience. 2021. V. 24. № 11. P. 103291. doi: 10.1016/j.isci.2021.103291

3 Ghosh S., Moreira M.V.B., Fantini C., González J.C. Growth and optical properties of nanocrystalline Sb_2 Se_3 thin-films for the application in solar-cells // Solar Energy. 2020. V. 211. P. 613–621. doi: 10.1016/j.solener.2020.10.001

4 Nolas G.S., Sharp J., Goldsmid J. Thermoelectrics: basic principles and new materials developments. Springer Science & Business Media, 2013. V. 45. doi: 10.1007/978–3–662–04569–5

5 Goldsmid H.J. Bismuth telluride and its alloys as materials for thermoelectric generation // Materials. 2014. V. 7. №4. P. 2577–2592. doi: 10.3390/7042577

6 Scherrer H., Scherrer S. Bismuth telluride, antimony telluride, and their solid solutions // CRC Handbook of thermoelectrics. CRC Press, 2018. P. 211-238.

7 Yang W., Kim J.H., Hutter O.S. Benchmark performance of low-cost Sb_2 Se_3 photocathodes for unassisted solar overall water splitting // Nature Communications. 2020. V 11. № 1. P. 861. doi: 10.1038/s41467–020–14704–3

8 Sankapal B.R., Lokhande, C.D. Photoelectrochemical characterization of Bi2Se3 thin films deposited by SILAR technique // Materials Chemistry and Physics. 2002. V. 73. № 2–3. P. 151–155. doi: 10.1016/s0254–0584(01)00362–5

9 Li W., Deng L., Wang X., Cao J. et al. Close-spaced thermally evaporated 3D Sb_2 Se_3 film for high-rate and high-capacity lithium-ion storage // Nanoscale. 2021. V. 13. № 21. P. 9834–9842. doi: 10.1039/d1nr01585k

10 Xue M.–Z., Fu Z.–W. Pulsed laser deposited Sb_2 Se_3 anode for lithium-ion batteries // J. Alloys Compd. 2008. V. 458. P. 351–356. doi: 10.1016/j.jallcom.2007.03.109

11 Zhang H., Liu C.–X., Qi X.–L., Dai X. et al. Topological insulators in Bi_2 Se_3, Bi_2 Te_3 and Sb_2 Te_3 with a single Dirac cone on the surface // Nature Physics. 2009. V. 5. P. 438–442.

12 Mazumder K., Shirage P.M. A brief review of $Bi_2 Se_3$ based topological insulator: From fundamentals to applications // Journal of Alloys and Compounds. 2012. V. 888. № 25. P. 161492. doi: 10.1016/j.jallcom.2021.161492

13 Anversa J., Chakraborty S., Piquini P., Ahuja R. High pressure driven superconducting critical temperature tuning in $Sb_2 Se_3$ topological insulator // Appl. Phys. Lett. 2016. V. 108. P. 212601. doi: 10.1063/1.4950716

14 Zhang K., Xu M., Li N., Xu M. et al. Superconducting Phase Induced by a Local Structure Transition in Amorphous Sb2Se3 under High Pressure // Phys. Rev. Lett. 2021. V. 127. № 12. P. 127002. doi: 10.1103/PhysRevLett.127.127002

15 Ioffe A.F. Semiconductor Thermoelements and Thermoelectric Cooling. A.F. Ioffe. London: Infosearch Limited, 1957. 1923p.

16 Suh J., Yu K.M, Fu D., Liu X. et al. Simultaneous enhancement of electrical conductivity and thermopower of $Bi_2 Te_3$ by multifunctionality of native defects // Adv. Mater. 2015. V. 27. № 24. P. 3681–3686. doi: 10.1002/adma.201501350

17 Shchurova M.A., Andreev O.V., Kuznetsova A.V. Electrophysical properties of the BI_{2-X} SE_{3-X}-X SMSE alloys as thermoelectric converter of n-type // Tyumen state university herald. 2013. V. 5. P. 82–87.

18 Yapryntsev M., Vasiliev A., Ivanov O. Sintering temperature effect on thermoelectric properties and microstructure of the grained Bi1.9Gd0.1Te3 compound // J. Eur. Ceram. Soc. 2019. V. 39. № 4. P. 1193–1205. doi: 10.1016/j.jeurceramsoc.2018.12.041

19 Ivanov O., Yaprintsev M., Lyubushkin R., Soklakova O. Enhancement of thermoelectric efficiency in $Bi_2 Te_3$ via rare earth element doping // Scr. Mater. 2018. V. 146. P. 91–94. doi: 10.1016/j.scriptamat.2017.11.031Get rights and content

20 Yaprintsev M., Lyubushkin R., Soklakova O., Ivanov O. Effects of Lu and Tm doping on thermoelectric properties of $Bi_2 Te_3$. // J. Electron. Mater. 2018. V. 47. № 2. P. 1362–1370. doi: 10.1007/s11664–017–5940–8

21 Ivanov O., Yaprintsev M. Mechanisms of thermoelectric efficiency enhancement in Lu-doped $Bi_2 Te_3$. // Mater. Res. Express. 2018. V. 5. № 1. P. 1–10. doi: 10.1088/2053–1591/aaa265

22 Yapryntsev M.N., Lyubushkin R.A., Soklakova O.N. Synthesis and electrical properties of Bi_2Te_3-based thermoelectric materials doped with Er, Tm, Yb, and Lu // Semiconductors. 2017. V. 51. № 6. P. 710–713. doi: 10.1134/S106378261706029X

23 Yang J.J., Wu F.F., Zhu Z.Z., Yao L.L. et al. Thermoelectrical properties of lutetium-doped $Bi_2 Te_3$ bulk samples prepared from flower-like nanopowders // J. Alloys Compd. 2015. V. 619. P. 401–405. doi: 10.1016/J.JALLCOM.2014.09.024

24 Singh N., Schwingenschlogl U. $LaBiTe_3$: An unusual thermoelectric material // Phys. Status RRI. 2014. V. 8. № 9. P. 805–808. doi: 10.1002/pssr.201409110

25 Lin. J., Vanderbilt D. Weyl semimetals from noneentrosymmetric topological insulators // Physical Review B. 2014. V. 90. № 15. P. 155–316. doi: 10.1103/PhysRevB.90.155316

26 Li Zh., Si Ch., Zhou J., Xu H. et al. Yttrium-Doped $Sb_2 Te_3$: A Promising Material for Phase-Change Memory // ACS Appl. Mater. Interfaces. 2016. V. 8. № 39. P. 26126–26134. doi: 10.1021/acsami.6b08700

27 Yaprintseva M., Vasil'eva A., Ivanova O. Thermoelectric properties of the textured Bi1.9Gd0.1Te3 compounds sparkplasma-sintered at various temperature // Journal of the European Ceramic Society. 2020. V. 40. № 3. P. 742–775. doi: 10.1016/j.jeurceramsoc.2019.11.028

28 Yarembash E.I., Eliseev A.A. Chalcogenides of rare earth elements. M: Nauka, 1975, 260 p.

29 Ghosh G. The Sb-Te (Antony-Tellurium) system // Journal of Phaze Equilibria. 1994. V. 15. P. 349–360.

30 Eckerbin V.P., Stegher A. On the phases in the Sb-Te system // Acta Crystallo-graphica. 1966. V. 2. P. 78.

31 Brown A., Liewis B. The systems bismuth-tellurium and antimony – tellurium and synthesis of the antimony – tellurium and the synthesis of the minerals hedleyite and wehrlite // Journal of Physics and Chemistry of Solids. 1962. V. 23. P. 1597–1604.

32 Sadigov F.M., Alizade N.M., Ismailov Z.I. Nature of chemical interaction in the ternal system Er-Bi (Sb) – Se // Eurasian Union of Scientists. 2021. V. 1. P. 82.

33 Sadigov F.M., Mammadova S.H., Ismayilov Z.I. State diagram of Er-Sb system // Ganja. 2022. P. 85–87.

34 Лякишева Н.П. Диаграммы состояния бинарных металлических систем. Справочник М.: Машиностроение, 1997. 1023 с.

References

1 Baghbanzadeh-Dezfuli B., Jamali-Sheini F., Cheraghizade M. Sonical deposition of nanostructured Sb2 Se3 films for optoelectronic applications. Journal of Alloys and Compounds. 2021. vol. 85. no. 1. pp. 157308. doi: 10.1016/j.jallcom.2020.157308

2 Wang F.K., Yang S.J., Zhai T.Y. 2D Bi2 Se3 materials for optoelectronics. IScience. 2021. vol. 24. no. 11. pp. 103291. doi: 10.1016/j.isci.2021.103291

3 Ghosh S., Moreira M.V.B., Fantini C., González J.C. Growth and optical properties of nanocrystalline Sb2 Se3 thin-films for the application in solar-cells. Solar Energy. 2020. vol. 211. pp. 613–621. doi: 10.1016/j.solener.2020.10.001

4 Nolas G.S., Sharp J., Goldsmid J. Thermoelectrics: basic principles and new materials developments. Springer Science & Business Media, 2013. vol. 45. doi: 10.1007/978–3–662–04569–5

5 Goldsmid H.J. Bismuth telluride and its alloys as materials for thermoelectric generation. Materials. 2014. vol. 7. no. 4. pp. 2577–2592. doi: 10.3390/7042577

6 Scherrer H., Scherrer S. Bismuth telluride, antimony telluride, and their solid solutions. CRC Handbook of thermoelectrics. CRC Press, 2018. pp. 211-238.

7 Yang W., Kim J.H., Hutter O.S. Benchmark performance of low-cost Sb2 Se3 photocathodes for unassisted solar overall water splitting. Nature Communications. 2020. vol. 11. no. 1. pp. 861. doi: 10.1038/s41467–020–14704–3

8 Sankapal B.R., Lokhande, C.D. Photoelectrochemical characterization of Bi2Se3 thin films deposited by SILAR technique. Materials Chemistry and Physics. 2002. vol. 73. no. 2–3. pp. 151–155. doi: 10.1016/s0254–0584(01)00362–5

9 Li W., Deng L., Wang X., Cao J. et al. Close-spaced thermally evaporated 3D Sb2 Se3 film for high-rate and high-capacity lithium-ion storage. Nanoscale. 2021. vol. 13. no. 21. pp. 9834–9842. doi: 10.1039/d1nr01585k

10 Xue M.–Z., Fu Z.–W. Pulsed laser deposited Sb2 Se3 anode for lithium-ion batteries. J. Alloys Compd. 2008. vol. 458. pp. 351–356. doi: 10.1016/j.jallcom.2007.03.109

11 Zhang H., Liu C.–X., Qi X.–L., Dai X. et al. Topological insulators in Bi2 Se3, Bi2 Te3 and Sb2 Te3 with a single Dirac cone on the surface. Nature Physics. 2009. vol. 5. pp. 438–442.

12 Mazumder K., Shirage P.M. A brief review of Bi2 Se3 based topological insulator: From fundamentals to applications. Journal of Alloys and Compounds. 2012. vol. 888. no. 25. pp. 161492. doi: 10.1016/j.jallcom.2021.161492

13 Anversa J., Chakraborty S., Piquini P., Ahuja R. High pressure driven superconducting critical temperature tuning in Sb2 Se3 topological insulator. Appl. Phys. Lett. 2016. vol. 108. pp. 212601. doi: 10.1063/1.4950716

14 Zhang K., Xu M., Li N., Xu M. et al. Superconducting Phase Induced by a Local Structure Transition in Amorphous Sb2Se3 under High Pressure. Phys. Rev. Lett. 2021. vol. 127. no. 12. pp. 127002. doi: 10.1103/PhysRevLett.127.127002

15 Ioffe A.F. Semiconductor Thermoelements and Thermoelectric Cooling. A.F. Ioffe. London, Infosearch Limited, 1957. 1923p.

16 Suh J., Yu K.M, Fu D., Liu X. et al. Simultaneous enhancement of electrical conductivity and thermopower of Bi2 Te3 by multifunctionality of native defects. Adv. Mater. 2015. vol. 27. no. 24. pp. 3681–3686. doi: 10.1002/adma.201501350

17 Shchurova M.A., Andreev O.V., Kuznetsova A.V. Electrophysical properties of the BI2-X SE3-X-X SMSE alloys as thermoelectric converter of n-type. Tyumen state university herald. 2013. vol. 5. pp. 82–87.

18 Yapryntsev M., Vasiliev A., Ivanov O. Sintering temperature effect on thermoelectric properties and microstructure of the grained Bi1.9Gd0.1Te3 compound. J. Eur. Ceram. Soc. 2019. vol. 39. no. 4. pp. 1193–1205. doi: 10.1016/j.jeurceramsoc.2018.12.041

19 Ivanov O., Yaprintsev M., Lyubushkin R., Soklakova O. Enhancement of thermoelectric efficiency in Bi2 Te3 via rare earth element doping. Scr. Mater. 2018. vol. 146. pp. 91–94. doi: 10.1016/j.scriptamat.2017.11.031Get rights and content

20 Yaprintsev M., Lyubushkin R., Soklakova O., Ivanov O. Effects of Lu and Tm doping on thermoelectric properties of Bi2 Te3. J. Electron. Mater. 2018. vol. 47. no. 2. pp. 1362–1370. doi: 10.1007/s11664–017–5940–8

21 Ivanov O., Yaprintsev M. Mechanisms of thermoelectric efficiency enhancement in Lu-doped Bi2 Te3. Mater. Res. Express. 2018. vol. 5. no. 1. pp. 1–10. doi: 10.1088/2053–1591/aaa265

22 Yapryntsev M.N., Lyubushkin R.A., Soklakova O.N. Synthesis and electrical properties of Bi2Te3-based thermoelectric materials doped with Er, Tm, Yb, and Lu. Semiconductors. 2017. vol. 51. no. 6. pp. 710–713. doi: 10.1134/S106378261706029X

23 Yang J.J., Wu F.F., Zhu Z.Z., Yao L.L. et al. Thermoelectrical properties of lutetium-doped Bi2 Te3 bulk samples prepared from flower-like nanopowders. J. Alloys Compd. 2015. vol. 619. pp. 401–405. doi: 10.1016/J.JALLCOM.2014.09.024

24 Singh N., Schwingenschlogl U. LaBiTe3: An unusual thermoelectric material. Phys. Status RRI. 2014. vol. 8. no. 9. pp. 805–808. doi: 10.1002/pssr.201409110

25 Lin. J., Vanderbilt D. Weyl semimetals from noneentrosymmetric topological insulators. Physical Review B. 2014. vol. 90. no. 15. pp. 155–316. doi: 10.1103/PhysRevB.90.155316

26 Li Zh., Si Ch., Zhou J., Xu H. et al. Yttrium-Doped Sb2 Te3: A Promising Material for Phase-Change Memory. ACS Appl. Mater. Interfaces. 2016. vol. 8. no. 39. pp. 26126–26134. doi: 10.1021/acsami.6b08700

27 Yaprintseva M., Vasil'eva A., Ivanova O. Thermoelectric properties of the textured Bi1.9Gd0.1Te3 compounds sparkplasma-sintered at various temperature. Journal of the European Ceramic Society. 2020. vol. 40. no. 3. pp. 742–775. doi: 10.1016/j.jeurceramsoc.2019.11.028

28 Yarembash E.I., Eliseev A.A. Chalcogenides of rare earth elements. M, Nauka, 1975, 260 p.

29 Ghosh G. The Sb-Te (Antony-Tellurium) system. Journal of Phaze Equilibria. 1994. vol. 15. pp. 349–360.

30 Eckerbin V.P., Stegher A. On the phases in the Sb-Te system. Acta Crystallo-graphica. 1966. vol. 2. pp. 78.

31 Brown A., Liewis B. The systems bismuth-tellurium and antimony – tellurium and synthesis of the antimony – tellurium and the synthesis of the minerals hedleyite and wehrlite. Journal of Physics and Chemistry of Solids. 1962. vol. 23. pp. 1597–1604.

32 Sadigov F.M., Alizade N.M., Ismailov Z.I. Nature of chemical interaction in the ternal system Er-Bi (Sb) – Se. Eurasian Union of Scientists. 2021. vol. 1. pp. 82.

33 Sadigov F.M., Mammadova S.H., Ismayilov Z.I. State diagram of Er-Sb system. Ganja. 2022. pp. 85–87.

34 Lyakisheva N.P. State diagrams of binary metal systems. Handbook M., Mechanical Engineering, 1997. 1023 p. (in Russian).

Сведения об авторах

Saba H. Mamadova Cand. Sci. (Chem.), associate professor, general and inorganic chemistry department, Baku State University, Azerbaijan, 23 Zahid Khalilov street, Baku Az1148, Azerbaijan, saba.mammadova36@gmail.com
https://orcid.org/0000-0002-6545-2070

Fuad M. Sadigov Dr. Sci. (Chem.), professor, general and inorganic chemistry department, Baku State University, Azerbaijan, 23 Zahid Khalilov street, Baku Az1148, Azerbaijan, fuad.sadiqov.55@mail.ru
https://orcid.org/0009-0006-0571-6800

Zakir I. Ismailov Cand. Sci. (Chem.), associate professor, general and inorganic chemistry department, Baku State University, Azerbaijan, Azerbaijan, 23 Zahid Khalilov street, B, zakir-51@mail.ru
https://orcid.org/0000-0003-3499-953X

Information about authors

Саба Г. Мамадова к.х.н., доцент, кафедра общей и неорганической химии, Бакинский государственный университет, ул. Захида Халилова 23, Баку, Az1148, Азербайджан, saba.mammadova36@gmail.com
https://orcid.org/0000-0002-6545-2070

Фуад М. Садыгов доктор химических наук, профессор, кафедра общей и неорганической химии, Бакинский государственный университет, ул. Захида Халилова 23, Баку, Az1148, Азербайджан, fuad.sadiqov.55@mail.ru
https://orcid.org/0009-0006-0571-6800

Закир И. Исмаилов к.х.н., доцент, кафедра общей и неорганической химии, Бакинский государственный университет, ул. Захида Халилова 23, Баку, Az1148, Азербайджан, zakir-51@mail.ru
https://orcid.org/0000-0003-3499-953X

Kseniya B. Kim Cand. Sci. (Chem.), associate professor, inorganic chemistry and chemical technology department, Voronezh State University of Engineering Technologies, Voronezh, Russian Federation, avenue Revolution, 19, Voronezh, 394036, Russia, kmkseniya@yandex.ru
https://orcid.org/0000-0001-5564-8267
Sabukhi I. Niftaliyev Dr. Sci. (Chem.), professor, inorganic chemistry and chemical technology department, Voronezh State University of Engineering Technologies, Voronezh, avenue Revolution, 19, Voronezh, 394036, Russia, sabukhi@gmail.com
https://orcid.org/0000-0001-7887-3061

Ксения Б. Ким к.х.н., доцент, кафедра неорганической химии и химической технологии, Воронежский государственный университет инженерных технологий, пр-т Революции, 19, Воронеж, Россия, kmkseniya@yandex.ru
https://orcid.org/0000-0001-5564-8267

Сабухи И. Нифталиев д.х.н., профессор, заведующий кафедрой неорганической химии и химической технологии, Воронежский государственный университет инженерных технологий, пр-т Революции, 19, Воронеж, Россия, sabukhi@gmail.com
https://orcid.org/0000-0001-7887-3061

Вклад авторов

Все авторы в равной степени принимали участие в написании рукописи и несут ответственность за плагиат

Contribution

All authors are equally involved in the writing of the manuscript and are responsible for plagiarism

Конфликт интересов

Авторы заявляют об отсутствии конфликта интересов.

Conflict of interest

The authors declare no conflict of interest.

Поступила 04/07/2024	**После редакции** 22/07/2024	**Принята в печать** 12/08/2024

Received 04/07/2024	**Accepted in revised** 22/07/2024	**Accepted** 12/08/2024